Droplet Impaction on a Supersonic Wedge: Consideration of Similitude

L. J. Forney*
Georgia Institute of Technology, Atlanta, Georgia

The theoretical collection efficiency has been determined for water droplets impinging on a two-dimensional supersonic wedge with an attached shock. By defining a moving coordinate system such that the gas is stationary behind the shock and scaling the droplet Stokes number with a shock-to-wedge distance, a similarity parameter has been defined that properly accounts for the effects of freestream Mach number, wedge angle, and large-droplet Reynolds number. The effective Stokes number, which represents the ratio of the droplet stopping distance in the moving frame to the appropriate shock-to-wedge length, is shown to correlate both the total collection efficiency and the local impingement rate.

Nomenclature

C = wedge length, cm
C_D = droplet drag coefficient
d_p = droplet diameter, cm
E = total droplet collection efficiency
ℓ = shock-to-wedge length, cm
ℓ' = shock-to-wedge length, cm
ℓ'' = distance measured along shock wave, cm
ℓ''' = distance measured along shock wave, cm
M_1 = freestream gas Mach number
R = gas constant, $cm^2/s^2 - K$
Re = local droplet Reynolds number, $=\rho_2 U d_p/\mu_2$
Re_0 = initial droplet Reynolds number, $=\rho_2 V_1 d_p/\mu_2$
Re_1 = freestream droplet Reynolds number, $=\rho_1 V_1 d_p/\mu_2$
Re_2 = droplet Reynolds number, $=\rho_2 V_2 d_p/\mu_2$
s = distance along surface, cm
T = wedge thickness, cm, $=2T_{1/2}$
$T(s)$ = local wedge thickness, cm, $=2s(\sin\sigma)$
T_1 = freestream static temperature
$T_{1/2}$ = wedge thickness, cm
$T_{1/2}(s)$ = local wedge thickness, cm
t = time, s
U = local droplet velocity, cm/s
U_2 = initial droplet velocity behind shock, cm/s
V_1 = freestream gas velocity, cm/s
V_2 = gas velocity behind shock
W = droplet mass incident on wedge, g/s
x = droplet displacement in moving frame, cm
x_m = maximum droplet displacement in moving frame, cm
x_p = reference length, cm
β = local droplet impingement rate
γ = ratio of specific heats
ε = empirical constant, $=0.158$
ζ = initial droplet displacement from wedge centerline, cm
η = distance along wedge surface, cm
η' = distance traveled by moving frame, cm, $=V_2 t$
θ = angle of shock wave
μ_1 = freestream viscosity of gas, g/cm-s
μ_2 = gas viscosity behind shock, g/cm-s
ν = angle between $\bar{V}_1$ and $\bar{U}_2$
ρ_1 = freestream gas density, g/cc
ρ_2 = gas density behind shock, g/cc
σ = wedge semiapex angle
τ = droplet relaxation time, s
Ψ = modified Stokes number
Ψ_s = local modified Stokes number
Ψ_0 = Stokes number
Ω = ratio of gas velocities, $=V_2/V_1$
ω = freestream droplet mass per unit volume, g/cc

I. Introduction

DURING supersonic flight, small differences in airfoil profile due to ice accumulation will create large changes in flying characteristics. The possibility of ice accumulation on aircraft missiles traveling at supersonic speeds exists at flight Mach numbers up to 1.4.[1] At large Mach numbers, aerodynamic heating will prevent icing, but at low supersonic speeds and ambient temperatures, icing will occur. Moreover, ice may accumulate on exposed surfaces even if the stagnation temperature of the ambient dry air is above freezing because of depressed temperatures on wet surfaces due to latent heat exchange.[2] Other interest in the trajectories of particles and droplets near exposed surfaces in supersonic flight may be associated with the potential for surface erosion and ablation.[3]

Regardless of the flight speed, the potential for ice buildup or surface erosion depends on knowledge of cloud droplet trajectories and impingement rates from theoretical calculations or experiments. In the present paper, the analysis of Serafini[1] has been extended for the case of droplet impingement on two-dimensional wedges with attached shocks, as shown in Fig. 1. A simplified analysis is provided for the derivation of analytical expressions for the equation of droplet trajectories. More importantly, a droplet Stokes number or similarity parameter is defined that correlates all of Serafini's results for both the total rate and distribution of droplet impingement. This scaling parameter will be useful in attempts to correlate either theoretical or experimental data for the impaction of droplets or particles on other airfoil shapes.

Serafini, in his pioneering work, modified the droplet stopping distance and thus the Stokes number to include the effects of large-droplet Reynolds number. These results were recently shown by Israel and Rosner[4,5] to be useful in the correlation of the collection efficiencies on spheres and cylin-

Received Oct. 5, 1987; revision received Oct. 20, 1988. Copyright © 1989 American Institute of Aeronautics and Astronautics, Inc. All rights reserved.

*Associate Professor, School of Chemical Engineering.

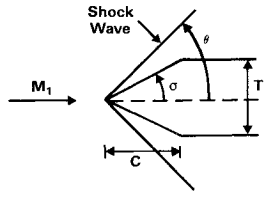

Fig. 1 Attached shock on wedge of small angle.

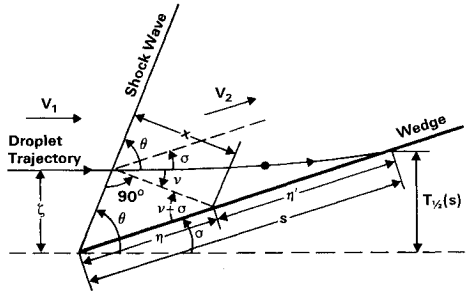

Fig. 2 Schematic of droplet trajectory.

ders in subsonic flows. Modifications to the droplet Stokes number also have been useful to predict the capture efficiencies of aerosol particles in granular beds at low Reynolds numbers.[6] Probstein and Fassio[3] demonstrated that the collection efficiency in the stagnation region of a cylinder or sphere reduced to a single curve in hypersonic flow if the particle Stokes number was rescaled with the shock detachment distance.

II. Droplet Trajectory

Serafini considered wedge semiapex angles covering the range 1.14–6.84 deg. For these wedge angles, the shock-wave-attachment Mach number varies from a value slightly greater than 1 to roughly 1.4. The shock wave angle θ and the semiapex angle $\sigma = \tan^{-1}(T/2C)$, where T and C are the wedge thickness and length, respectively, are indicated in the schematic of Fig. 1.

For simplicity, as assumed in previous work, the water drops are spherical, the flow behind the shock is a frictionless perfect gas with constant heat capacity, and the effects of droplet heat and mass transfer are negligible. Moreover, since the air velocity behind the shock wave in Figs. 1 and 2 is constant and parallel to the wedge surface, a frame of reference is adopted that moves at the constant air velocity V_2 behind the shock.[1] Hence, relative to the moving frame, the droplet is projected across the shock wave into quiescent air.

The trajectory of a single droplet approaching a wedge at a distance ζ from the centerline is illustrated in Fig. 2. After the droplet crosses the shock, it is deflected by the gas behind the shock wave until it impacts on the wedge. In the moving frame of reference, however, the droplet must travel a distance x to the wedge surface perpendicular to the shock wave. The distance x also represents the relative displacement of the droplet to the gas behind the shock.

The point of impaction of the droplet at a distance s along the wedge surface from the leading edge is therefore the vectorial sum of the droplet displacement x within the moving frame of reference and the displacement of the moving frame ($=V_2 t$) over the same interval of time. Thus, one derives a parametric equation for 1) the distance of the droplet from the centerline ζ, and 2) the distance s along the wedge to the point of impaction. The parametric equations are

$$\zeta = x \sin\theta \tan(\nu + \sigma) \tag{1}$$

$$s = x \sec(\nu + \sigma) + V_2 t \tag{2}$$

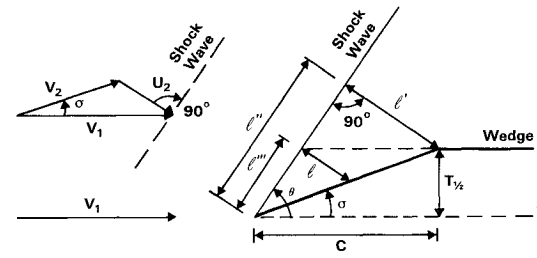

Fig. 3 Geometry of shock-to-wedge length ℓ.

where $\nu = \pi/2 - \theta$ and the shock wave angle θ is tabulated as a function of σ.[7]

III. Equations of Motion

The equation of motion of a droplet projected into a region of quiescent air is

$$\frac{dU}{dt} = -\frac{3}{4}\left(\frac{\rho}{\rho_d}\right)\left(\frac{U^2}{d_p}\right) C_D \tag{3}$$

where U is the particle velocity, ρ the gas density, and C_D the drag coefficient. In the moving frame of reference behind the shock wave, the initial velocity of the droplet is

$$U_2 = |\bar{V}_1 - \bar{V}_2| \tag{4}$$

as indicated in Fig. 3, where $\bar{U}$ is normal to the shock wave from consideration of momentum conservation across the oblique shock.

In the present paper, the analysis of the displacement of the water droplet x behind the shock wave in the moving frame of reference is simplified by writing

$$\frac{dU}{dx} = \left(\frac{dU}{dt}\right)\left(\frac{1}{U}\right) \tag{5}$$

or

$$x = \int_{U_2}^{U} \frac{U\, dU}{(dU/dt)} \tag{6}$$

Rewriting the droplet velocity U in Eqs. (3) and (6) in terms of a local Reynolds number $Re = (d_p U \rho_2/\mu_2)$ where ρ_2 and μ_2 are the gas density and viscosity behind the shock wave in Fig. 2 and substituting, Eq. (6) becomes

$$x = \frac{4}{3}\frac{d_p \rho_p}{\rho_2} \int_{Re}^{Re_0} \frac{dRe'}{(Re')C_D(Re')} \tag{7}$$

where

$$Re_0 = \frac{\rho_2 U_2 d_p}{\mu_2}$$

In Eq. (7), non-Stokesian drag on the droplet is assumed by adopting a drag coefficient of the form[1,8,9]

$$C_D = \frac{24}{Re}(1 + \varepsilon Re^{2/3}) \tag{8}$$

where $\varepsilon = 0.158$. Thus, the expression for the droplet displacement in the moving frame of reference becomes

$$x = x_p\left[Re_0^{1/3} - Re^{1/3} + \left(\frac{1}{\varepsilon^{1/2}}\right)\tan^{-1}(Re^{1/3}\varepsilon^{1/2}) - \left(\frac{1}{\varepsilon^{1/2}}\right)\tan^{-1}(Re_0^{1/3}\varepsilon^{1/2})\right] \tag{9}$$

where $x_p = (d_p/6\varepsilon)(\rho_p/\rho_2)$. In addition, the maximum droplet displacement $x_m = \lim_{Re\to 0} x$ becomes

$$x_m = x_p\left[Re_0^{1/3} - \frac{1}{\varepsilon^{1/2}}\tan^{-1}(Re_0^{1/3}\varepsilon^{1/2})\right] \tag{10}$$

A similar analysis relating the time for droplet displacement to a local droplet Reynolds number is derived from

$$t = \int_{U_2}^{U} \frac{dU}{(dU/dt)} \tag{11}$$

or integrating, one finds

$$t = \tau\ell n\left[\left(\frac{Re_0}{Re}\right)^{2/3}\left(\frac{1+\varepsilon Re^{2/3}}{1+\varepsilon Re_0^{2/3}}\right)\right] \tag{12}$$

where $\tau = (d_p^2\rho_p/12\mu_2)$.

IV. Total Collection Efficiency

The total droplet collection efficiency of the wedge represents the fraction of droplets that impact on the surface of those that are geometrically incident. Thus, the total collection efficiency is defined as

$$E = 2\zeta_u/T \tag{13}$$

where ζ_u is the initial displacement from the leading edge (normal to the freestream) of the droplet trajectory that impinges at the shoulder of the wedge.

It is possible to determine the collection efficiency E by specifying the following variables: droplet diameter d_p, density ρ_p, wedge velocity V_1, freestream gas density ρ_1, static temperature T_1, semiapex angle σ, and wedge thickness T. These variables determine the freestream droplet Reynolds number $Re_1 = (\rho_1 V_1 d_p/\mu_1)$ and gas Mach number $M_1 = V_1\sqrt{\gamma RT_1}$. From knowledge of the gas Mach number and freestream droplet Reynolds number, one obtains the initial droplet Reynolds number in the moving frame, since

$$\frac{Re_0}{Re_1} = \left(\frac{\rho_2}{\rho_1}\right)\left(\frac{\mu_1}{\mu_2}\right)\left(\frac{U_2}{V_1}\right) \tag{14}$$

where

$$\frac{U_2}{V_1} = (1 + \Omega^2 - 2\Omega\cos\sigma)^{1/2} \tag{15}$$

Substituting Re_0 into Eqs. (9) and (12) and noting that $s = (T/2)\csc\sigma$, one obtains ζ_u from the parametric equations (1) and (2).

Serafini correlated the total collection efficiency E with a Stokes number Ψ_0 defined by

$$\Psi_0 = \frac{x_m}{2C} \tag{16}$$

where x_m is the droplet stopping distance defined by Eq. (10). One correlation is shown in Fig. 4 for fixed Mach number $M_1 = 1.3$ and wedge thickness ratio $\tan\sigma = 0.06$. The droplet diameters covered in Fig. 4 range from 2 to 100 μ, and the ambient conditions correspond to a supersonic wedge at an altitude of 4.57 km. Thus, the freestream droplet Reynolds number Re_1 in Fig. 4 varies from 42 to 2104.

The correlation of Fig. 4 demonstrates that the effects of non-Stokesian drag on the droplet are properly accounted for by the impaction or similarity parameter defined by Eq. (16). The Stokes number defined by Eq. (16) was also recently used to successfully correlate impaction data on cylinders and spheres in subsonic streams under conditions of large particle Reynolds numbers.[4]

Serafini also plotted values of the total collection efficiency E vs Stokes number Ψ_0 for conditions of varying wedge thickness ratios covering values between 0.02 and 0.12, as shown in Fig. 5, and for gas Mach numbers varying between 1.1 and 2.0, as indicated in Fig. 6. Clearly, the Stokes number Ψ_0 does not properly account for the effects of the wedge geometry or the freestream Mach number on the total collection efficiency.

V. Similitude

Historically, particle collection efficiencies on collectors of various shapes (e.g., spheres, cylinders, or airfoils) in subsonic flows ($M_1 \ll 1$) have been correlated with a Stokes number defined as the ratio of the particle or droplet stopping distance to a characteristic collector dimension.[1,9] In the absence of a collector dimension, e.g., particle capture at a stagnation point, the characteristic dimension is replaced by the appropriate ratio of freestream velocity to local velocity gradient.[4,9]

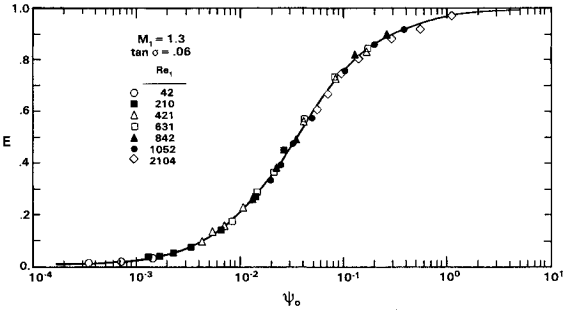

Fig. 4 Total droplet collection efficiency vs Stokes number. Freestream gas conditions $\rho_1 = 0.82 \times 10^{-3}$ g/cc and $T_1 = 262$ K.

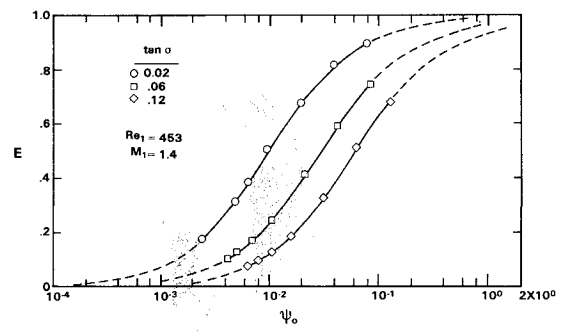

Fig. 5 Total droplet collection efficiency vs Stokes number indicating effect of wedge semiapex angle.

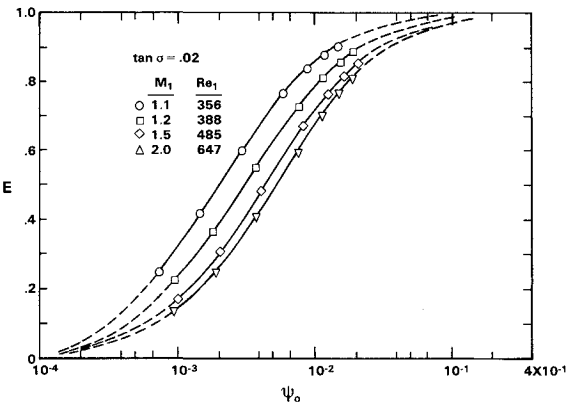

Fig. 6 Total droplet collection efficiency vs Stokes number indicating effect of freestream Mach number.

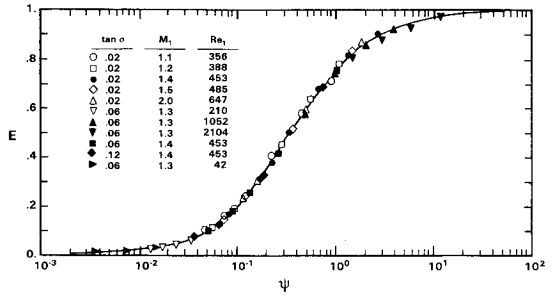

Fig. 7 Total droplet collection efficiency vs modified Stokes number.

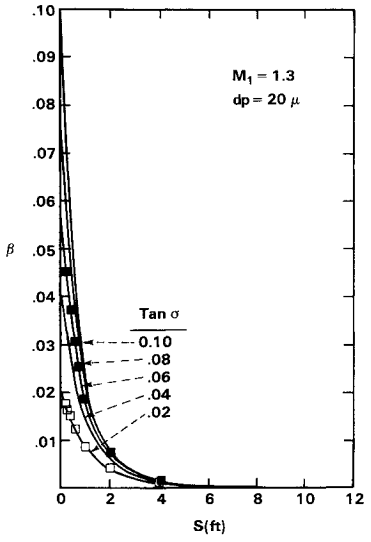

Fig. 8 Local impingement efficiency vs distance along surface.

If the stream is supersonic, however, recent theoretical calculations of the particle collection efficiency of a cylindrical probe aligned parallel to the freestream suggest that the shock detachment distance is the characteristic length with which to scale the particle stopping distance.[3,8] Referring to Fig. 3, the shock-to-wedge length ℓ measured perpendicular to the shock wave is the appropriate dimension in the present problem. Clearly, if the droplet stopping distance x_m in the moving frame of reference is much greater than ℓ, the droplet collection efficiency on the supersonic wedge would approach one.

Thus, substituting the shock-to-wedge length ℓ for the wedge length C in the definition of the droplet Stokes number, one writes

$$\Psi = \Psi_0 \left(\frac{C}{\ell'}\right)\left(\frac{\ell'}{\ell}\right) \tag{17}$$

From the geometry of Fig. 3,

$$\frac{\ell'}{\ell} = \frac{\ell''}{\ell'''} \tag{18}$$

where

$$\sin\theta = \frac{T_{1/2}}{\ell'''} \tag{19}$$

$$\tan(\theta - \sigma) = \frac{\ell}{\ell''} \tag{20}$$

Hence, substituting Eqs. (19) and (20) into Eq. (18), one has

$$\frac{\ell'}{\ell} = \frac{\ell' \sin\theta}{T_{1/2}\tan(\theta - \sigma)} \tag{21}$$

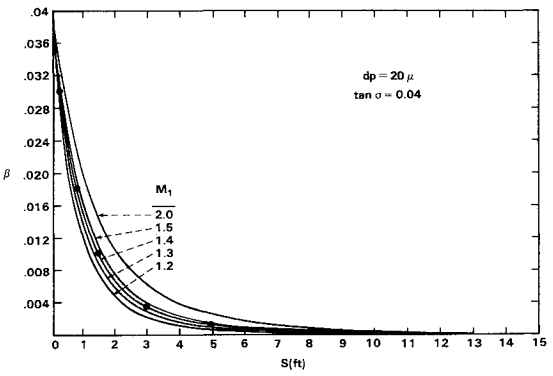

Fig. 9 Local impingement efficiency vs distance along surface.

Rewriting Eq. (17), one therefore obtains a modified similarity parameter or Stokes number of the form

$$\Psi = \left(\frac{x_m}{T}\right)\frac{\sin\theta}{\tan(\theta - \sigma)} \tag{22}$$

The collection efficiency data presented in Figs. 4–6 was replotted as a function of the modified Stokes number Ψ, and the results are shown in Fig. 7. Clearly, the similarity parameter Ψ defined by Eq. (22) properly accounts for the wedge geometry and the effects of gas compressibility on the total droplet collection efficiency.

VI. Local Impingement Rate

The local rate of impingement of droplets on the wedge or airfoil surface is important in terms of the potential for icing. An analytical expression of the local rate of impingement can be obtained from expressions for ζ and s. The normalized rate of accumulation of droplets per unit area of surface is defined by the expression[1]

$$\beta = \frac{d\zeta}{ds} = \frac{d\zeta/dRe}{ds/dRe} \tag{23}$$

Differentiating Eqs. (1) and (2), one obtains

$$\frac{d\zeta}{ds} = \frac{\sin\theta\tan(v+\sigma)}{\sec(v+\sigma) + V_2\left(\dfrac{dt/dRe}{dx/dRe}\right)} \tag{24}$$

or

$$\beta = \frac{\sin\theta\tan(v+\sigma)}{\sec(v+\sigma) + \dfrac{V_2}{U}} \tag{25}$$

It should be noted that the limiting value of β at the leading edge of the wedge where $U = U_2$ is obtained from the vectorial geometry of $\bar{V}_1$, $\bar{V}_2$, and $\bar{U}_2$ such that

$$\lim_{s\to 0}\beta = \sin\sigma \tag{26}$$

The preceding expressions for β and s can be solved parametrically in terms of droplet Reynolds number Re, where $V_2/U = Re_2/Re$ in Eq. (25). These solutions provide contours of local impingement rate β vs distance s along the wedge surface.[1] Serafini explored the effects of freestream gas Mach number M_1, droplet diameter d_p, and wedge thickness ratio on the local impingement rate β (see Figs. 8–10).

It is now instructive to derive an expression for the local impingement rate β by considering the total collection efficiency on a wedge surface of length s. The total mass of water in the freestream incident on a wedge surface of length

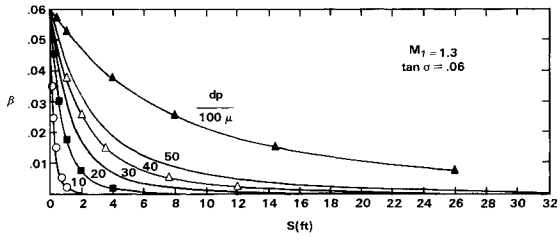

Fig. 10 Local impingement efficiency vs distance along surface.

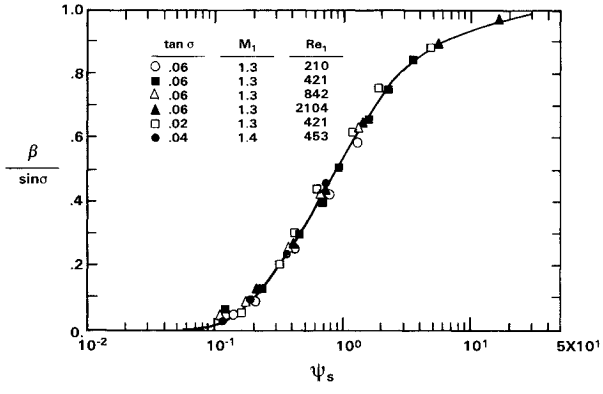

Fig. 11 Local impingement efficiency vs local modified Stokes number.

s as shown in Fig. 2 is

$$W = \omega V_1(\sin\sigma)s \tag{27}$$

where ω is the mass per unit volume of water droplets in the freestream. Therefore, the total mass of water impinging on the wedge surface of length s is $WE(\Psi_s)$, where $E(\Psi_s)$ is the total collection efficiency and Ψ_s is a local value of the modified Stokes number defined by Eq. (22), or

$$\Psi_s = \left(\frac{x_m}{T(s)}\right)\frac{\sin\theta}{\tan(\theta-\sigma)} \tag{28}$$

and $T(s) = 2s(\sin\sigma)$.

The normalized local impingement rate β is now defined as

$$\beta = \left(\frac{1}{\omega V_1}\right)\frac{d}{ds}[WE(\Psi_s)] \tag{29}$$

Writing the derivative of Eq. (29) in the form

$$\frac{d}{ds}[WE(\Psi_s)] = E\left(\frac{dW}{ds}\right) + W\left(\frac{dE}{d\Psi_s}\right)\left(\frac{d\Psi_s}{ds}\right) \tag{30}$$

and substituting Eqs. (29) and (28), one obtains

$$\beta = \sin\sigma\left[E(\Psi_s) - \Psi_s\left(\frac{dE(\Psi_s)}{d\Psi_s}\right)\right] \tag{31}$$

Thus, the local impingement rate becomes

$$\frac{\beta}{\sin\sigma} = f(\Psi_s) \tag{32}$$

The local impingement rate data of Figs. (8–10) were plotted in the form of Eq. (32), and these results are shown in Fig. 11. It is apparent, as in the case of Fig. 7, that a local value of the modified Stokes parameter Ψ_s properly accounts for the effects of wedge thickness ratio and gas compressibility on the local droplet impingement rate.

VII. Summary

Universal curves representing the total collection efficiency and the local impingement rate, respectively, have been predicted for droplets impinging on a two-dimensional supersonic wedge with an attached shock. To accomplish this, a modified droplet Stokes number has been defined that represents the ratio of the droplet stopping distance to the appropriate shock-to-wedge length. This similarity parameter is shown to account properly for the effects of freestream Mach number, wedge angle, and large-droplet Reynolds number. It is expected that a similar approach would be useful in the correlation of droplet impaction data of either experimental or numerical results for other geometries such as cones or flat plates.

Acknowledgment

The author wishes to thank D. E. Rosner of Yale University for his complete review of the manuscript and for bringing the work of Probstein and Fassio to his attention.

References

[1]Serafini, J. S., "Impingement of Water Droplets on Wedges and Double-Wedge Airfoils at Supersonic Speeds," NACA TN 1159, 1954.

[2]Tribus, M. and Guibert, A., "Impingement of Spherical Water Droplets on a Wedge at Supersonic Speeds in Air," *Journal of Aerospace Science*, Vol. 19, No. 6, 1952, pp. 391–394.

[3]Probstein, R. F. and Fassio, F., "Dusty Hypersonic Flows," *AIAA Journal*, Vol. 8, No. 4, 1970, pp. 770–779.

[4]Israel, R. and Rosner, D. E., "Use of a Generalized Stokes Number to Determine the Aerodynamic Capture Efficiency of Non-Stokesian Particles from a Compressible Gas Flow," *Aerosol Science and Technology*, Vol. 2, No. 1, 1983, pp. 45–51.

[5]Wessel, R. A. and Righi, J., "Generalized Correlations for Inertial Impaction of Particles on a Circular Cylinder," *Aerosol Science and Technology*, Vol. 9, No. 1, 1988, pp. 29–60.

[6]D'Ottavio, T. and Goren, S. L., "Aerosol Capture in Granular Beds in the Impaction Dominated Regime," *Aerosol Science and Technology*, Vol. 2, No. 2, 1983, pp. 91-108.

[7]Neice, M. M., "Tables and Charts of Flow Parameters Across Oblique Shocks," NACA TN 1673, 1948.

[8]Forney, L. J. and McGregor, W. K., "Particle Sampling in Supersonic Streams with a Thin-Walled Cylindrical Probe," *AIAA Journal*, Vol. 25, No. 8, 1987, pp. 1100–1104.

[9]Friedlander, S. K., *Smoke, Dust and Haze: Fundamentals of Aerosol Behavior*, Wiley, New York, 1976.